

# Strongly-Driven One-Atom Laser

P. Lougovski<sup>1</sup>, F. C. Casagrande<sup>2</sup>, A. Lulli<sup>2</sup> and E. Solano<sup>3,4</sup>

<sup>1</sup>Hearne Institute for Theoretical Physics, Department of Physics and Astronomy,  
Louisiana State University, 202 Nicholson Hall, Baton Rouge, LA 70803, USA

<sup>2</sup>Dipartimento di Fisica, Università di Milano, Via Celoria 16, 20133 Milano, Italy

<sup>3</sup>Physics Department, ASC, and CENS, Ludwig-Maximilians-Universität, Theresienstrasse 37, 80333 Munich, Germany

<sup>4</sup>Sección Física, Departamento de Ciencias, Pontificia Universidad Católica del Perú, Apartado 1761, Lima, Peru

(Dated: December 16, 2019)

We propose the implementation of a strongly-driven one-atom laser, based on the  $\omega$ -resonant interaction of a three-level atom in  $\omega$ -cavity with a single cavity mode and three laser fields. We show that the system can be described equivalently by a two-level atom coupled to the cavity and driven by a strong effective coherent field, yielding Schrödinger cat states. The effective dynamics can be solved exactly, including a thermal field bath, allowing an analytical description of field statistics and entanglement properties, as well as of the environment-induced decoherence of atom-field pure states. Finally, we propose a way to monitor the decoherence of these states by measuring atomic populations and confirm the validity of our model through full numerical solutions.

PACS numbers: 42.50.Fx, 42.50.Vk, 73.21.La

## I. INTRODUCTION

In cavity quantum electrodynamics (CQED) the interaction between atoms and photons can be investigated experimentally under carefully controlled conditions, and described by relatively simple models [1]. These features make CQED an almost ideal framework to investigate the foundations of quantum mechanics and their application to quantum information [2]. For instance, two-atom entanglement [3] as well as the entanglement between an atom and a photon [4] have been recently demonstrated. On the other hand, the basic interaction between a two-level atom and a cavity field mode, as described by the Jaynes-Cummings (JC) model [5], leads to nonclassical effects carefully tested in recent years [6]. Furthermore, it allowed the implementation of the micromaser [7] and the microlaser [8] in the strong coupling regime of CQED, in the microwave and optical domain, respectively. Further efforts led to the implementation of a trapped ion as a nanoscopic probe of cavity field modes [9]. More recently, a single trapped neutral atom in a high-Q optical cavity [10] allowed the implementation of a one-atom laser [11], i.e., lasing with only one intra-cavity atom. These systems can exhibit features that are not present in standard macroscopic lasers such as thresholdless generation and sub-Poissonian photon statistics [12].

Another milestone in CQED experiments was reached in Ref. [13], where a "Schrödinger cat" state of the cavity field, a mesoscopic superposition of two coherent states, was realized. There, the field decoherence was monitored through atom-atom correlation measurements. State reconstruction of nonclassical intra-cavity fields was also possible through atom-cavity dispersive interactions [14, 15]. More recently, a remarkable proposal for the resonant generation of Schrödinger cat states [16] was implemented in the lab [17], and tested with the help of a quantum spin-echo technique [18]. The understanding of entanglement in atom-cavity systems was

enhanced when an additional driving field acting on the cavity mode was added on top of the atom-cavity JC interaction [19, 20]. In this respect, recently, an elegant analysis of a driven cavity containing a two-level atom explained the absence or increase of entanglement in the transient of the atom-cavity dynamics [21]. Unfortunately, most realistic models including dissipative processes require numerical analysis, or ideal theoretical conditions for the sake of semi-analytical derivations.

In this work, we introduce an integrable model of a strongly-driven one-atom laser (SDOAL) where the coherent driving field acts directly on the atom. We consider a realistic model consisting of a three-level atom in  $\omega$ -cavities placed inside a single-mode optical cavity, coupled  $\omega$ -resonantly to three coherent laser fields. We show that this model can be reduced to two atomic levels coupled to a cavity mode and a strong classical driving on the atom, yielding Schrödinger cat states. In this strong-driving limit [22], we solve the full system dynamics [23], in the transient and in the steady state, providing one more of the few examples of an exactly solvable open quantum system. In previous works [24, 25], we developed related results for microwave cavity fields and two-level Rydberg atoms, not a good model for a field in the optical regime and fast decaying atomic dipolar transitions. Here, we solve analytically the master equation for the full atom-field system in the SDOAL model. Next, we exploit the obtained solutions for the analysis of atom-field entanglement and the decoherence of atom-field superposition states via the measurement of atomic populations. Finally, we present numerical results confirming the validity of the approximation made to derive the effective master equation of the SDOAL model.

The paper is organized as follows. In section II we introduce the integrable model of a SDOAL. In section III we solve analytically the master equation for the atom-cavity dynamics. In section IV we describe entanglement properties and the environment-induced decoherence of

the SD O A L, presenting a scheme to monitor decoherence via atom ic populations measurements. A numerical analysis that confirms the validity of the model is presented in section V. Conclusions are reported in section VI.

## II. THE STRONGLY DRIVEN ONE-ATOM LASER MODEL

We consider a three-level atom (ion) in a configuration trapped inside an optical cavity (Fig. 1). We assume that the transition  $|3\rangle \leftrightarrow |2\rangle$  is quadrupolar and, hence, the metastable states  $|3\rangle$  and  $|2\rangle$  cannot be coupled directly, but only via the level  $|1\rangle$ . The level  $|1\rangle$  can decay via spontaneous emission and, therefore, the external lasers and the cavity field are all far detuned with respect to the corresponding transition frequencies. We suppose that the atom interacts off-resonantly with a single mode of a cavity field of a frequency  $\omega_f$  on the transition  $|3\rangle \leftrightarrow |2\rangle$ . The same transition is coupled off-resonantly to a coherent field of a frequency  $\omega_1^0$ . The remaining atom ic transition  $|3\rangle \leftrightarrow |1\rangle$  is coupled off-resonance to two lasers of frequency  $\omega_1^0$  and  $\omega_2^0$ . The different frequency detunings,  $\Delta$  and  $\Delta'$ , of these two processes prevent the system from undesired transitions.

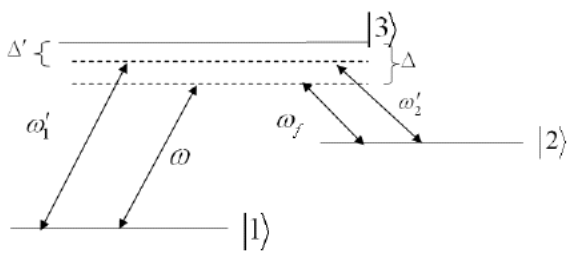


FIG. 1: A tom ic energy levels and the applied elds. and  $\Delta$  denote the frequency detunings,  $\omega_f$  is the frequency of the cavity mode, and  $\omega_1^0, \omega_2^0, \omega$  are the frequencies of the lasers applied to the associated transitions.

We assume, without loss of generality, that both the cavity mode coupling frequency  $g$  and the associated laser Rabi frequencies  $\omega_1^0, \omega_2^0$  are real. The Ham iltonian  $\hat{H}(t)$  for the whole system can be written as  $\hat{H}(t) = \hat{H}_0 + \hat{H}_1(t)$ , where

$$\hat{H}_0 = \sim \omega_3 \hat{S}^{33} + \sim \omega_2 \hat{S}^{22} + \sim \omega_1 \hat{S}^{11} + \sim \omega_f \hat{a}^\dagger \hat{a}; \quad (1)$$

$$\begin{aligned} \hat{H}_1(t) = & \sim g (\hat{a}^\dagger \hat{S}^{23} + \hat{a} \hat{S}_+^{23}) + \sim (e^{-i\omega_1^0 t} \hat{S}_+^{13} + e^{i\omega_1^0 t} \hat{S}^{13}) \\ & + \sim \omega_1^0 (e^{-i\omega_1^0 t} \hat{S}_+^{13} + e^{i\omega_1^0 t} \hat{S}^{13}) \\ & + \sim \omega_2^0 (e^{-i\omega_2^0 t} \hat{S}_+^{23} + e^{i\omega_2^0 t} \hat{S}^{23}); \end{aligned} \quad (2)$$

Here  $\hat{a}$  ( $\hat{a}^\dagger$ ) is the cavity mode annihilation (creation) operator and, following the notation of [26], we define

the atom ic operators as follows,

$$\begin{aligned} \hat{S}_+^{23} &= \hat{p}_{ih2} \hat{S}^{23} = \hat{p}_{ih3} \hat{S}_+^{13} = \hat{p}_{ih1} \hat{S}^{13} \\ \hat{S}^{13} &= \hat{p}_{ih3} \hat{S}^{13} = \hat{p}_{ihJ} \hat{S}^{13} \quad (J = 1, 2, 3); \end{aligned} \quad (3)$$

We rewrite the Ham iltonian  $\hat{H}(t)$  in the interaction picture leaving the unavoidable time dependence in the term related to the laser Rabi frequency

$$\begin{aligned} \hat{H}_i(t) = & \sim \hat{S}_+^{22} \sim \hat{S}_+^{11} \sim (\hat{a}^\dagger \hat{a}^\dagger \hat{a} \hat{a}) \\ & + \sim g \left[ \left( \hat{a} + \frac{1}{2} \right) \hat{S}_+^{23} + h.c. \right] \\ & + \sim \omega_1^0 \left[ \left( 1 + \frac{1}{2} e^{i(\Delta - \omega_1^0 t)} \right) \hat{S}_+^{13} + h.c. \right]; \end{aligned} \quad (4)$$

If  $\omega_1^0, \omega_2^0, \Delta$  are real, the unitary dynamics of the atom - eld system in Eq. (4) can be described by an effective Ham iltonian for a two-level atom coupled to the cavity mode and in presence of a classical driving eld. This is due to the fact that, under these conditions, the energy diagram of Fig. 1 can be understood as composed by two independent -schemes. In this case, it is straightforward to prove that we can build the second-order Ham iltonian

$$\hat{H}_e = \sim g_e (\hat{a}^\dagger \hat{S}_+^{12} + \hat{a} \hat{S}^{12}) \sim g_e (\hat{S}_+^{12} + \hat{S}^{12}); \quad (5)$$

with  $g_e = g$  and  $\omega_e = \omega_1^0 - \omega_2^0$ . In Eq. (5), as is usually done, we have assumed the compensation of constant AC Stark-shift terms by a proper retuning of the laser frequencies. The Stark-shift term depending on the intracavity photon number can be neglected if  $g_e$ . In the strong-driving limit,  $g_e = g$ , as explained in Ref. [22], we can derive the effective Ham iltonian

$$\hat{H}_e = \frac{g_e}{2} (\hat{a}^\dagger + \hat{a}) (\hat{S}_+^{12} + \hat{S}^{12}); \quad (6)$$

We have tested numerically the above analytical considerations and proved, in fact, that Eq. (6) describes the correct effective dynamics.

However, we want to show here that we can go beyond the limit of uncoupled -schemes and obtain a similar dynamics with less demanding conditions on the experimental parameters. To prove this statement we exploit the small rotations method of Ref. [26], which is essentially a perturbative method for deriving effective Ham iltonians. First, we introduce the operators of a SU(3) deformed algebra,

$$\begin{aligned} \hat{X}_+^{23} &= \left( \hat{a} + \frac{1}{2} \right) \hat{S}_+^{23}; \quad \hat{X}^{23} = \left( \hat{a}^\dagger + \frac{1}{2} \right) \hat{S}^{23}; \\ \hat{Y}_+^{13} &= b_c \hat{S}_+^{13}; \quad \hat{Y}^{13} = b_c \hat{S}^{13}, \end{aligned} \quad (7)$$

where  $b_c = 1 + \frac{1}{2} e^{i(\Delta - \omega_1^0 t)}$ . Using the identity relation  $\hat{f} = \hat{S}^{11} + \hat{S}^{22} + \hat{S}^{33}$  we can rewrite the interaction Ham iltonian Eq. (4) in the compact form,

$$\begin{aligned} \hat{H}_i(t) = & \sim \hat{S}_+^{22} \sim \hat{S}_+^{11} \sim (\hat{a}^\dagger \hat{a}^\dagger \hat{a} \hat{a}) \\ & + \sim g (\hat{X}_+^{23} + \hat{X}^{23}) + \sim \omega_1^0 (\hat{Y}_+^{13} + \hat{Y}^{13}); \end{aligned} \quad (8)$$

We can eliminate the dependence of  $\hat{H}_i$  on the upper level  $\beta_i$  by applying two consecutive small rotations. The first unitary transformation  $\hat{U}^{13} = \exp(-\hat{Y}_+^{13} - \hat{Y}^{13})g$ , with  $\hat{g} = \frac{1}{\sqrt{2}}(1 - \hat{\beta}_i)$  and the condition  $(\hat{g})^2 = 1$ , allows us to eliminate the dependence on operators  $\hat{Y}^{13}$ . The second unitary small rotation, given by  $\hat{U}^{23} = \exp(-\hat{X}_+^{23} - \hat{X}^{23})g$ , with  $\hat{g} = \frac{1}{\sqrt{2}}(1 - \hat{\beta}_i)$  and the conditions  $(\hat{g})^2 = 1$ ,  $(\hat{g})^2 = 1$ , can be used to eliminate the dependence on  $\hat{X}^{23}$ . After some lengthy algebra we derive the effective two-level Hamiltonian

$$\hat{H}_e^0 = \sim(\hat{S}_+^{22} + \sim(\hat{S}_+^{12} + \hat{S}^{12})) \sim_e (\hat{S}_+^{12} + \hat{S}^{12}); \quad (9)$$

where we introduced the effective coupling and driving frequencies  $g_e = \frac{g_e}{\sqrt{2}}$  and  $\omega_e = \frac{\omega_e}{\sqrt{2}}$ . Note that the above derivation does not depend on the order of the two small rotations. The effective Hamiltonian (9) is exact to zero-th order in the diagonal terms and to first-order in the other ones. From now on we shall consider the case of small detuning difference  $\omega_e \ll \omega_0$ , such that the diagonal terms are negligible. This will allow us to obtain an exactly solvable model of system dynamics even in the presence of dissipation, that is a one-atom laser. Hence, the initial model described by the Hamiltonian of Eqs. (1) and (2) reduces to a Hamiltonian that exhibits an effective coupling of the states  $|j_1i\rangle$  and  $|j_2i\rangle$  to the cavity mode according to an anti-Jaynes-Cummings interaction in the presence of a classical external field driving the atomic transition. Now we can apply the unitary transformation  $\hat{U} = \exp(-i\omega_e(\hat{S}_+^{12} + \hat{S}^{12}))t$  to obtain [22]

$$\hat{H}_e^0 = \frac{g_e}{2} [(\hat{j}_1^+ i\hat{n}_1 + \hat{j}_1^- i\hat{n}_1) + e^{2i\omega_e t} (\hat{j}_2^+ i\hat{n}_2 + \hat{j}_2^- i\hat{n}_2)]; \quad (10)$$

where we used the eigenstates  $|j_i\rangle = \frac{|j_1\rangle + |j_2\rangle}{\sqrt{2}}$  of the operator  $\hat{S}_x = \hat{S}_+^{12} + \hat{S}^{12}$ . In this way, we put in evidence fast rotating terms in Eq. (10) and, after applying the RWA with  $\omega_e \ll g_e$ , we obtain the simple effective Hamiltonian

$$\hat{H}_e = \frac{g_e}{2} (\hat{a}^y + \hat{a}) (\hat{S}_+^{12} + \hat{S}^{12}); \quad (11)$$

This Hamiltonian has the structure of resonant and simultaneous Jaynes-Cummings and anti-Jaynes-Cummings interactions [22] and its dynamics is better understood in terms of Schrödinger cat states than Rabi oscillations, as will be discussed later. Note that the Hamiltonian of Eq. (11) is similar to the one of Eq. (6) but with a more relaxed set of parameters. Furthermore, the dynamics is fully confirmed by numerical simulations.

To describe the open atom-cavity system dynamics we must include the dissipative effects due to the coupling of the cavity to the environment. We note that the decay of the upper level  $\beta_i$  can be neglected because of the elimination procedure described above. Therefore,

the system dynamics can be described by the following SDOAL master equation (ME)

$$\dot{\hat{a}}_F = -\frac{i}{\gamma} [\hat{H}_e; \hat{a}_F] + \hat{L}_{AF}; \quad (12)$$

where the dissipative term is the standard Liouville superoperator for a damped harmonic oscillator

$$\hat{L}_{AF} = -\frac{1}{2} (\hat{a}^y \hat{a}_F + 2\hat{a}_F \hat{a}^y + \hat{a}_F \hat{a}^y \hat{a}); \quad (13)$$

Here,  $\gamma$  is the cavity photon decay rate and we consider the limit of zero temperature because the system operates in the optical regime. However, the same analytical developments could be done in presence of a finite temperature bath.

### III. ANALYTICAL SOLUTION OF THE SDOAL MASTER EQUATION

The time evolution of the atom-field system is described by the density operator  $\hat{\rho}_F(t)$  which is the solution of the ME in Eq. (12). In order to solve it, we introduce the following decomposition

$$\hat{\rho}_F(t) = \hat{j}_1^+ i\hat{n}_1 \hat{j}_1^- i\hat{n}_1 \hat{j}_2^+ i\hat{n}_2 \hat{j}_2^- i\hat{n}_2 + \hat{j}_1^+ i\hat{n}_1 \hat{j}_3^+ i\hat{n}_3 \hat{j}_2^+ i\hat{n}_2 \hat{j}_4^+ i\hat{n}_4 \hat{j}_1^- i\hat{n}_1 \hat{j}_3^- i\hat{n}_3 \hat{j}_2^- i\hat{n}_2 \hat{j}_4^- i\hat{n}_4; \quad (14)$$

Here,  $\hat{j}_i^{\pm} i\hat{n}_i$  ( $i = 1, \dots, 4$ ) are operators describing the cavity field defined as

$$\begin{aligned} \hat{j}_1^+ i\hat{n}_1 &= \hat{h}^+ \hat{j}_AF(t) \hat{j}_1^+ i; & \hat{j}_2^+ i\hat{n}_2 &= \hat{h}^+ \hat{j}_AF(t) \hat{j}_2^+ i; \\ \hat{j}_3^+ i\hat{n}_3 &= \hat{h}^+ \hat{j}_AF(t) \hat{j}_3^+ i; & \hat{j}_4^+ i\hat{n}_4 &= \hat{h}^+ \hat{j}_AF(t) \hat{j}_4^+ i; \end{aligned} \quad (15)$$

Then, the master equation (12) is equivalent to the following set of equations for the operators  $\hat{j}_i^{\pm} i\hat{n}_i$

$$\dot{j}_1^+ i\hat{n}_1 = \frac{g_e}{2} [\hat{a}^y + \hat{a}]; \quad \dot{j}_2^+ i\hat{n}_2 = \hat{L}_{1;2F}; \quad (16)$$

$$\dot{j}_3^+ i\hat{n}_3 = \frac{g_e}{2} f \hat{a}^y + \hat{a}; \quad \dot{j}_4^+ i\hat{n}_4 = \hat{L}_{3;4F}; \quad (17)$$

where brackets  $[\cdot]$  and braces  $f;g$  denote the standard commutator and anti-commutator symbols.

We assume that the initial atom-field density operator is  $\hat{\rho}_F(0) = \hat{j}_1^+ i\hat{n}_1 \hat{j}_1^- i\hat{n}_1$ . Therefore, operators  $\hat{j}_i^{\pm} i\hat{n}_i$  read

$$\hat{j}_i^{\pm} i\hat{n}_i(0) = \frac{1}{2} \hat{j}_1^+ i\hat{n}_1 \hat{j}_i^{\pm} i\hat{n}_i; \quad (i = 1, \dots, 4); \quad (18)$$

In order to solve Eqs. (16) and (17), we map them onto a set of first order partial differential equations for the functions  $j_i(\cdot; t) = T_{\hat{F}} [\hat{j}_i^{\pm} i\hat{n}_i \hat{D}(\cdot)]$ ,  $i = 1, \dots, 4$ , where  $\hat{D}(\cdot)$  denotes a displacement operator. The functions  $j_i(\cdot; t)$  cannot be interpreted as characteristic functions for the cavity field, because the operators  $\hat{j}_i^{\pm} i\hat{n}_i$  do not exhibit all required properties of a density operator. As a consequence the functions  $j_i(\cdot; t)$  do not fulfill all conditions

for quantum characteristic functions. Nevertheless, they are continuous and square-integrable, which is enough for our purposes. From Eqs. (16) and (17) we obtain the following set of partial differential equations,

$$\frac{\partial \psi_{1,2}}{\partial t} = \frac{ig_e}{2} ( + )_{1,2} - \frac{1}{2} j \frac{\partial}{\partial x} \psi_{1,2}; \\ \frac{1}{2} ( \frac{\partial}{\partial x} + \frac{\partial}{\partial y} ) \psi_{1,2} \quad (19)$$

$$\frac{\partial \psi_{3,4}}{\partial t} = ig_e ( \frac{\partial}{\partial x} - \frac{\partial}{\partial y} ) \psi_{3,4} - \frac{1}{2} j \frac{\partial}{\partial y} \psi_{3,4} \\ - \frac{1}{2} ( \frac{\partial}{\partial x} + \frac{\partial}{\partial y} ) \psi_{3,4}; \quad (20)$$

To solve these differential equations we use the method of characteristics, for which it is useful to rewrite them in terms of the real and imaginary parts of the complex variable  $= x + iy$ ,

$$\frac{\partial \psi_{1,2}}{\partial t} = ig_e x \psi_{1,2} - \frac{(x^2 + y^2)}{2} \psi_{1,2} - \frac{1}{2} (x \frac{\partial}{\partial x} + y \frac{\partial}{\partial y}) \psi_{1,2}; \quad (21)$$

$$\frac{\partial \psi_{3,4}}{\partial t} = ig_e \frac{\partial \psi_{3,4}}{\partial y} - \frac{(x^2 + y^2)}{2} \psi_{3,4} \\ - \frac{1}{2} (x \frac{\partial}{\partial x} + y \frac{\partial}{\partial y}) \psi_{3,4}; \quad (22)$$

If in the equations for  $\psi_{3,4}$  we introduce the shifted variable  $\tilde{y} = y - \frac{2g_{eff}}{k}$  the above equations can be written as

$$\frac{\partial \psi_{1,2}}{\partial t} + \frac{1}{2} (x \frac{\partial}{\partial x} + y \frac{\partial}{\partial y}) \psi_{1,2} = H_{1,2}(x; y) \psi_{1,2}; \quad (23)$$

$$\frac{\partial \psi_{3,4}}{\partial t} + \frac{1}{2} (x \frac{\partial}{\partial x} + y \frac{\partial}{\partial y}) \psi_{3,4} = H_{3,4}(x; y) \psi_{3,4} \quad (24)$$

where  $H_{1,2}(x; y) = x [F_1^0(x) - F_2^0(x)] + y G^0(y)$  and  $H_{3,4}(x; y) = y [E_1^0(y) - E_2^0(y)] + x D^0(x)$ . There, we have also introduced the derivatives of the following functions

$$F_1(x) = -\frac{x^2}{4}; \quad F_2(x) = ig_e x; \quad G(y) = -\frac{y^2}{4}; \\ E_1(y) = -\frac{y^2}{4}; \quad E_2(y) = 2g_e \left( \frac{g_e}{2} \ln y + y \right); \\ D(x) = -\frac{x^2}{4}; \quad (25)$$

With these definitions, together with the initial functions  $\psi_{i,0}(x; y) = i(x; y; 0)$  associated with the ones in Eq. (18), we can write the time-dependent solutions as

$$\psi_{1,2}(x; y; t) = \frac{1}{2} \exp \left( \frac{x^2 + y^2}{2} - 2i \frac{g_e}{2} x \right) [1 - e^{-\frac{t}{2}}] g; \quad (26)$$

$$\psi_{3,4}(x; y; t) = \frac{f(t)}{2} \exp \left( \frac{x^2 + y^2}{2} - 2i \frac{g_e}{2} y \right) [1 - e^{-\frac{t}{2}}] g; \quad (27)$$

where

$$f(t) = \exp \left( -\frac{g_{eff}^2}{2} t + 4 \frac{g_e^2}{2} (1 - e^{-t/2}) \right); \quad (28)$$

The most striking feature of the solutions for  $\psi_{3,4}$  in Eq. (27) is the presence of the factor  $e^{-\frac{g_{eff}^2}{2} t}$ , in contrast to the solutions for  $\psi_{1,2}$  in Eq. (26). This factor leads to the vanishing of functions  $\psi_{3,4}$  for sufficiently long times. To better understand the solutions (26) and (27) we rewrite them in terms of the complex variable

$$\psi_{1,2}(z; t) = \frac{1}{2} \exp \left( -\frac{j \frac{\partial}{\partial z}}{2} \right) [i_f(t) - i_r(t)]; \quad (29)$$

$$\psi_{3,4}(z; t) = \frac{f(t)}{2} \exp \left( -\frac{j \frac{\partial}{\partial z}}{2} \right) [i_f(t) + i_r(t)]; \quad (30)$$

where we have introduced the complex time-dependent function  $i_f(t) = ig_e (1 - e^{-t/2})$ . We immediately recognize that the operators  $i_f(t)$  corresponding to the functions  $\psi_{1,2}(z; t)$  are

$$i_{1F}(t) = \frac{1}{2} j(t) i_h(t) j; \\ i_{2F}(t) = \frac{1}{2} j(t) i_h(t) i_h(t) j; \\ i_{3F}(t) = \frac{1}{2} \frac{f(t)}{e^{2j(t)j^2}} j(t) i_h(t) i_h(t) j; \\ i_{4F}(t) = \frac{1}{2} \frac{f(t)}{e^{2j(t)j^2}} j(t) i_h(t) i_h(t) j; \quad (31)$$

In the limit of  $t \rightarrow 1$ , when the unitary dynamics dominates over the incoherent cavity dissipation, we can say that the state of the atom-field system is well approximated by the Schrödinger cat state

$$j(t)i_{AF} = \frac{1}{2} (j^+ i j^- (t) i + j^- i j^+ (t) i); \quad (32)$$

with  $\sim(t) = i \frac{g_{eff}}{2} t$ . On the other hand, the steady state of the atom-field system is the mixed state

$$i_{AF}^{ss} = \frac{j^+ i h^+ j_{1F}^{ss} + j^- i h^- j_{2F}^{ss}}{2} \\ = \frac{j^+ i h^+ j j^{ss} i h^{ss} j + j^- i h^- j j^{ss} i h^{ss} j}{2}; \quad (33)$$

with  $i_{AF}^{ss} = ig_e$ . The pure state  $j(t)i_{AF}$  turns into the mixture  $i_{AF}^{ss}$  at a rate  $2g_e^2 =$ . Therefore, in order to preserve quantum coherence in the atom-cavity system for longer times, it is desirable to choose the ratio  $g_e^2 =$  as small as possible. On the other hand, the size of the

coherent state  $j^{ss}i$  is given by the ratio  $g_e = \dots$ . If  $g_e = 1$  is too small then the state becomes nearly separable and the atom-cavity correlations mainly originate from the overlap in phase space of two small coherent states  $j^{ss}i$  and  $j^{-ss}i$ .

We consider next the reduced density operator for the cavity field  $\rho_F(t) = Tr_A[\rho_{AF}(t)] = \rho_{1F}(t) + \rho_{2F}(t)$ , where  $Tr_A$  denotes the partial trace over the atom field variables. We obtain from Eq. (31) the mixed state

$$\rho_F(t) = \frac{j_F(t)ih(t)j_F(t)ih(t)j_F(t)}{2} : \quad (34)$$

The cavity field mean photon number after an interaction time  $t$  is

$$\langle N \rangle_F(t) = Tr_F[\rho_F^2] = j_F(t)^2 = \frac{g_e^2}{2} (1 - e^{-\kappa t})^2 : \quad (35)$$

In the steady state the cavity field mean photon number is given by  $\langle N \rangle_{ss} = (g_e = 1)^2$ , that is, the squared ratio between the effective coupling frequency and the cavity decay rate, which rule the coherent and incoherent regimes of cavity field dynamics, respectively. The time-dependent photon statistics  $p_n(t)$  is given by a Poissonian distribution

$$p_n(t) = \frac{j_F(t)^{2n}}{n!} e^{-j_F(t)^2} : \quad (36)$$

Hence, at any time the photon statistics of the SDOAL is that of a coherent field, a natural consequence of tracing orthogonal atom field states  $j_i$ . Certainly, this will not be the case if we make a projective atom field measurement in the bare basis  $|j_1i, j_2i\rangle$  at a time  $t$  during the transient. Actually, after the atom measurement, the cavity field is in either of the pure states

$$\rho_F^{(1,2)}(t) = \frac{\rho_{1F}(t) + \rho_{2F}(t)}{2p_{1,2}(t)} \quad [3_F(t) + 4_F(t)] \quad (37)$$

where  $p_{1,2}(t)$  is the probability to find the atom in the state  $j_1i, j_2i$  respectively at a time  $t$  (see below). The corresponding photon statistics are

$$\begin{aligned} p_n^{(1,2)}(t) &= \ln j_F^{(1,2)}(t)j_i \\ &= \frac{1}{1 - f(t)} e^{-j_F(t)^2} \frac{j_F(t)^{2n}}{n!} \\ &= 1 - (1 - \frac{f(t)}{e^{-2j_F(t)^2}}) \end{aligned} \quad (38)$$

In the initial part of transient dynamics, for times  $t \ll 1/\kappa$ ,  $f(t) = \dots$  and the cavity field states are even and odd cat states

$$j_F^{(1,2)}(t) = \frac{j_1(t)i + j_2(t)i}{2(1 - e^{-2j_F(t)^2})} \quad (39)$$

As is well known [27], states as in Eq. (39) can exhibit quantum effects including oscillating photonstatistics,

sub Poissonian photonstatistics, and quadrature squeezing. In Fig. 2 we show the time behaviour of the Mandel-Fano parameter  $Q = \frac{\langle N^2 \rangle - \langle N \rangle^2}{\langle N \rangle}$  in both cases of atom detected in the lower ( $Q^{(1)}(t)$ ) and upper ( $Q^{(2)}(t)$ ) state and for different values of the steady state mean photon number. We see that  $Q^{(1)}(t)$  and  $Q^{(2)}(t)$  exhibit super and sub Poissonian photonstatistics, respectively, before approaching the steady state Poissonian distribution.

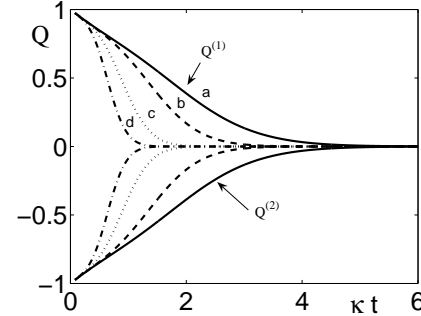


FIG. 2: The Mandel-Fano parameter  $Q$  for the cavity field versus dimensionless interaction time in the case of atom detected in the lower ( $Q^{(1)}(t)$ ) and upper ( $Q^{(2)}(t)$ ) states. We consider different values of the mean steady-state photon number  $\langle N \rangle_{ss}$ : (a) 1, (b) 2, (c) 5, (d) 10.

Now, we consider the reduced density operator for the atom  $\rho_A(t) = Tr_F[\rho_{AF}(t)]$ . From Eq. (31) we derive the following density matrix in the basis  $j_i$

$$\rho_A(t) = \frac{1}{2} \begin{pmatrix} 1 & f(t) \\ f(t) & 1 \end{pmatrix} : \quad (40)$$

From this atom field density matrix we can derive the probabilities  $p_{1,2}$  to find the atom in the lower or upper state,

$$p_{1,2}(t) = \frac{1}{2} [1 - f(t)] : \quad (41)$$

We observe that in the steady state the atom field population of the upper level  $j_2i$  is zero and those of the lower and intermediate levels are both equal to 0.5. The physical intuition behind this result is the orthogonality of coherent states  $j_1(t)i$  and  $j_2(t)i$  when  $t \neq 1/\kappa$ . We will employ these results in the following section to study the entanglement properties and the decoherence of the system.

#### IV. DECOHERENCE AND ENTANGLEMENT ANALYSIS

In section III, we presented a new scheme for generating atom-field superposition states [see Eq. (32)] in the transient regime and we described the steady state of a

SD O A L . Now, we evaluate atom - eld entanglement properties and show how to monitor the decoherence towards a steady state. We have shown in the preceding section that the state of the whole atom - eld system is almost a pure state on a time scale much shorter than the cavity decay time  $\tau = \hbar/k$ . Therefore, in this case, we can use the entropy of entanglement  $E(\rho)$  as an entanglement measure. It can be calculated in a straightforward way using the equality [2],

$$E(\rho) = S_A = S_F; \quad (42)$$

where  $S_A$  and  $S_F$  denote the von Neumann entropy of the atom ic and eld subsystems, respectively. The atom ic entropy reads

$$S_A = -f_1 \log_2 f_1 - f_2 \log_2 f_2; \quad (43)$$

where  $f_1, f_2$  are the eigenvalues of the reduced atom ic density matrix  $\rho_A(t)$ .

In the limit  $t \rightarrow 1$ , the atom ic density matrix in Eq. (40) can be approximated by

$$\rho_A(t) = \frac{1}{2} \begin{pmatrix} 1 & e^{2j\omega(t)t^2} \\ e^{-2j\omega(t)t^2} & 1 \end{pmatrix}; \quad (44)$$

whose eigenvalues are

$$f_{1,2}(t) = \frac{1}{2} \begin{pmatrix} 1 & \frac{i}{2} \\ 1 & e^{2j\omega(t)t^2} \end{pmatrix} = \frac{1}{2} \begin{pmatrix} 1 & \frac{i}{2} \\ 1 & e^{h\hat{N}i^{ss}(t)^2/2} \end{pmatrix}; \quad (45)$$

In Fig. 3 we plot the time evolution of the von Neumann

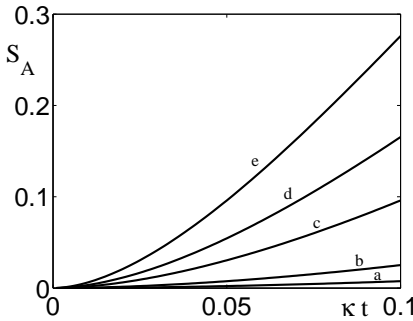


FIG. 3: The Von Neumann entropy  $S_A$  for the atom - eld system versus dimensionless time for different values of the mean steady-state photon number  $h\hat{N}i^{ss}$ : (a) 0.25, (b) 1, (c) 5, (d) 10, (e) 20.

entropy  $S_A$  for different values of the steady-state mean photon number  $h\hat{N}i^{ss}$ . We see that the system gets more entangled for larger values of  $h\hat{N}i^{ss}$ , i.e., when the ratio  $g_e/k$  is large. On the other hand, from the previous discussion it follows that such highly entangled atom - eld states are more fragile to the cavity decoherence since the decay rate of the coherence in the system is also ruled by  $h\hat{N}i^{ss}$ . The next important question to be answered is how to measure a decoherence rate in the atom - eld system, that is, how to determine the rate at which the atom - eld system reduces from a pure state to a statistical mixture. The environment-induced decoherence of

cavity eld superposition states has been both theoretically and experimentally studied in the case of high-Q microwave cavities [6]. There are several advantages for utilizing a microwave QED setup for these purposes. In particular, the lifetime of a photon in a microwave resonator is significantly longer than in an optical one. However, it is not possible to measure a microwave cavity eld directly, and the standard technique is to measure level population statistics for atoms passing through a cavity. In our case, we remark that the cavity eld reduced density operator does not depend on the function  $f(t)$ , so that we cannot reveal the decoherence of the entire system from measurements performed on the eld alone. However, a simple way to measure the decoherence rate of the atom - eld system is to detect the atom ic populations  $p_{1,2}$  of Eq. (41), which can be rewritten as

$$p_{1,2}(t) = \frac{1}{2} \begin{pmatrix} 1 & \exp[-2h\hat{N}i^{ss}t + 4h\hat{N}i^{ss}(1 - e^{-t/2})] \\ 1 & \end{pmatrix}; \quad (46)$$

Thus, by measuring/ fitting the atom ic populations  $p_{1,2}(t)$  for different evolution times  $t$ , we directly obtain the decoherence rate of the pure atom - eld state in the optical cavity

$$\gamma_D = 2h\hat{N}i^{ss} = \frac{g_e^2}{2}; \quad (47)$$

Assuming that we know  $g_e$  from initial calibration, we can also use the previous expression to estimate experimentally. Note that the decoherence rate  $\gamma_D$  may be larger than the dissipative decay rate  $\gamma$  depending on the value of the effective coupling frequency  $g_e$ . In the case of  $h\hat{N}i^{ss} = 0.25$  the two rates are equal. In Fig. (4) we illustrate the time evolution of  $p_1$  for different values of  $h\hat{N}i^{ss}$ . We see that the decoherence effects become relevant for values of  $h\hat{N}i^{ss} > 1$  as in the cases (d) and (e).

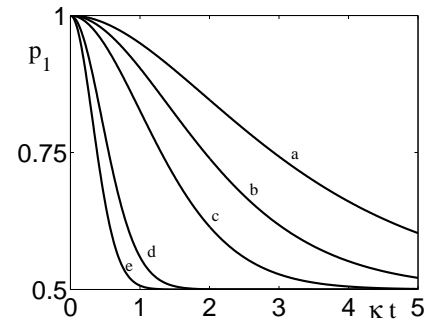


FIG. 4: Measurement of atom - cavity decoherence through population of the lower atom ic state  $|j\rangle$  versus dimensionless time evaluated for different values of  $h\hat{N}i^{ss}$ : (a) 0.25, (b) 0.5, (c) 1, (d) 5, (e) 10.

## V. NUMERICAL SIMULATIONS

In this section we discuss the theoretical approach presented in the above sections from a numerical point of

view. In fact, by means of a first order perturbative approach we have reduced the full three-level system dynamics to an effective two-level one described by the ME in Eq. (12). We now discuss the validity of that approximation for both Hamiltonian and dissipative dynamics.

In the numerical analysis we need to solve the full system ME

$$\hat{H}_{AF} = \frac{i}{\hbar} [\hat{H}_i(t); \hat{H}_{AF}] + \hat{L}_{AF}; \quad (48)$$

where the system Hamiltonian is given in Eq. (8) and the dissipative process is ruled by the Liouville super operator in Eq. (13). To solve Eq. (48) numerically we consider the dimensionless time  $\tilde{t} = t$  and the following dimensionless parameters

$$\begin{aligned} \tilde{\gamma}^0 &= \frac{0}{-}; \quad g = \frac{g}{-}; \quad \tilde{\gamma} = -; \quad \tilde{\gamma}_1^0 = \frac{0}{-1} \quad \tilde{\gamma}_2^0 = \frac{0}{-2} \\ \tilde{\gamma} &= -; \quad g_e = \frac{g}{\tilde{\gamma}_0}; \quad \tilde{\gamma}_e = \frac{\tilde{\gamma}_2^0 \tilde{\gamma}}{\tilde{\gamma}_0}; \end{aligned} \quad (49)$$

In order to solve the ME by means of the Monte Carlo Wave Function approach (MCWF) [28], we rewrite the ME in the Lindblad form to identify the collapse and the "free evolution" operators

$$\hat{H}_{AF} = \frac{i}{\hbar} (\hat{H}_e \hat{H}_{AF} - \hat{H}_{AF} \hat{H}_e^*) + \hat{C}_{AF} \hat{C}^* \quad (50)$$

where the non-Hermitian effective Hamiltonian  $\hat{H}_e$  is given by

$$\hat{H}_e = \frac{\hat{H}_i(t)}{2} - \frac{i\tilde{\gamma}}{2} \hat{C}^* \hat{C}; \quad (51)$$

and the only one collapse operator is  $\hat{C} = \hat{K}\hat{a}$ . The system dynamics can be simulated by a suitable number of trajectories, i.e. stochastic evolutions of the wave function  $j(t)$ , by means of the following main rule

$$j(t+\tau)i = \begin{cases} \frac{1}{p} \frac{\frac{1}{\hbar} \hat{H}_e(t) j(t)i}{1 - p(t)} & \text{if } p(t) < N_{rnd} \\ \frac{C_i j(t)i}{p(t)} & \text{if } p(t) > N_{rnd} \end{cases}; \quad (52)$$

where  $\tau$  is a suitable small time interval,  $p(t)$  is the collapse probability at time  $t$ , and  $N_{rnd}$  is a random number generated from a uniform distribution in  $[0;1]$ . We note that the collapse probability depends on the cavity field mean photon number  $\hat{N}_i(t)$  and can be evaluated as  $p(t) = \tau \hat{K} \hat{N}_i(t)$ . In the simulations we must consider parameters values in agreement with the theoretical conditions required by the two small rotations.

First we discuss the full three-level system Hamiltonian dynamics ( $K = 0$ ) in order to confirm the validity of the effective two-level Hamiltonian of Eq. (11). We consider the time evolution of the cavity field mean photon number and of the atomic populations, and we compare the numerical results with the theoretical expressions  $\hat{N}_i(t) = \frac{g_{eff}^2 t^2}{4}$ , and  $p_{1,2}(t) = \frac{1}{2} [1 - \exp(-\frac{g_{eff}^2 t^2}{2})]$ ,

$p_3(t) = 0$ . As an example, we show in Fig. 5 a case where the ratio of the effective parameters is  $\frac{g_{eff}}{g_e} = 25$ . We see a good agreement for the mean photon number (Fig. 5a). The theoretical functions  $p_{1,2}(t)$  are the envelopes of the numerical fast oscillating populations (Fig. 5b). In fact, in the numerical analysis we do not take into account the RWA approximation. In particular, the populations of levels  $j_1$  and  $j_2$  approach the expected value of 0.5, and the population of the upper level  $j_3$  is always negligible. In addition, we tested the prediction that the effective

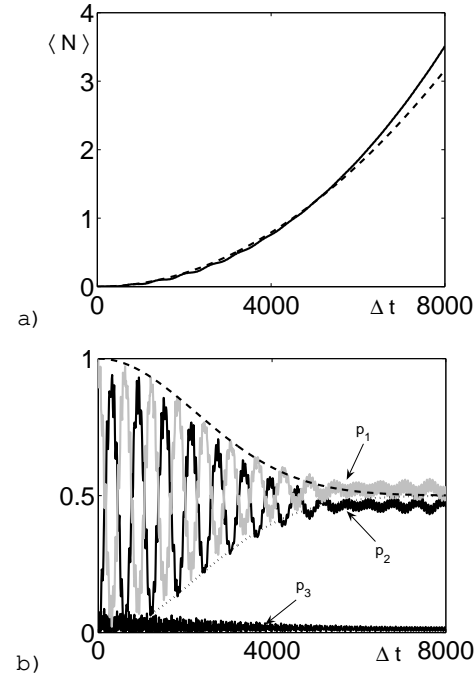


FIG. 5: Hamiltonian dynamics of the full three-level system for the parameters  $\tilde{\gamma}^0 = 0.9$ ,  $g = 0.004$ ,  $\tilde{\gamma} = 0.1$ ,  $\tilde{\gamma}_1^0 = 0.05$ ,  $\tilde{\gamma}_2^0 = 0.1$ . a) Cavity field mean photon number vs dimensionless time: numerical value (solid line) and theoretical value (dashed line). b) Atomic populations: numerical values (solid lines) and theoretical values (dashed lines).

dynamics allows to generate cavity field cat states when the atom is measured in level  $j_1$  or  $j_2$ . In Fig. 6 we show the Wigner function that describes in phase space the cavity field state prepared by an atom measurement in level  $j_1$  and we see the typical features of a cat state. Now we consider the full dynamics including dissipation of Eq. (48), for the same parameters as in Figs. 5, 6, and with  $K = g_e$ , so that we expect that the steady state value of mean photon number is one and it is reached in a time that is twice that of the atomic populations. In Fig. 7a we compare the numerical results for the time evolution of the cavity field mean photon number to the theoretical behavior predicted by Eq. (35), showing that there is a good agreement. In Fig. 7b we consider the numerically simulated time evolution of the atomic populations  $p_j(t)$  ( $j = 1, 2, 3$ ) compared to the theoretical functions in Eq. (46). We remark that the population of the upper level  $p_3(t)$  always remains negligible, the pop-

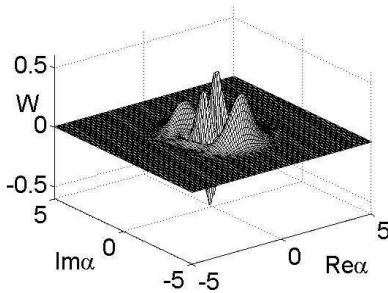


FIG. 6: Wigner function for the cavity field state after detection of the atom in the ground state [1]. The parameters are as in Fig. 5 and the dimensionless time is  $t = 7160$ .

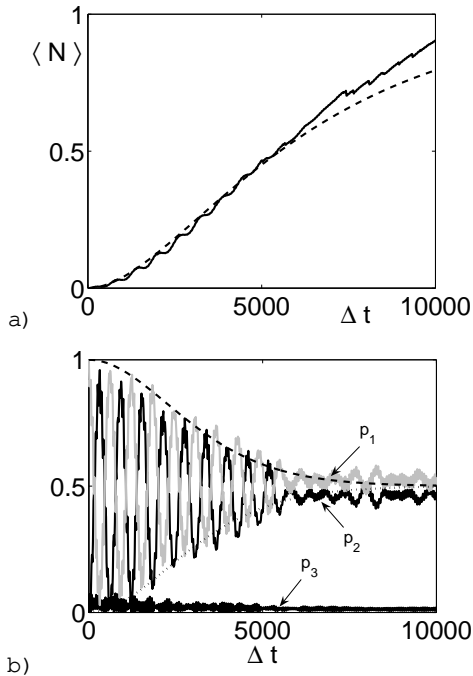


FIG. 7: Full dynamics of the three-level system for the parameters as in Fig. 5, and for  $K = g_e = 0.00044$ . a) Cavity field mean photon number vs dimensionless time: numerical value (solid line) and theoretical value (dashed line). b) Atom populations: numerical values (solid lines) and theoretical values (dashed lines). We used twenty trajectories.

ulations  $p_1(t)$  and  $p_2(t)$  reach the steady state value of 0.5, and the theoretical curves  $t$  the envelopes of the fast oscillating functions. The above results provide a clear demonstration of the validity of the two-level approximation developed in section II, which is at the basis of the subsequent theoretical developments.

## V I. CONCLUSIONS

We have introduced a solvable model of a SDQAL. We have shown analytically and numerically that the complex dynamics of a three-level atom, dispersively coupled to an optical cavity mode and to three laser fields, can be well described by a two-level atom that is resonantly coupled to a cavity mode and a strong coherent field. The initial transient regime shows that the system is approximately in an entangled atom-cavity field state, a Schrödinger cat state, whose entanglement can be described by the atomic von Neumann entropy. When decoherence mechanism becomes important, the system evolves to a mixed atom-field state until a final steady state. The cavity field is always in a mixed state whose photon statistics is Poissonian, while the atomic subsystem can exhibit coherences. If we measure the atomic state at a given time, we can project the cavity field in a nonclassical field with sub-Poissonian statistics. This is the key to monitor the whole atom-field decoherence. We propose a scheme for determining the system decoherence rate based on atomic population measurements. We find that the decoherence rate depends on the steady-state mean photon number, that is, on the ratio between an effective coupling frequency (a combination of coupling frequency, external laser amplitude and detuning parameter) and the dissipative cavity decay rate.

## VII. ACKNOWLEDGMENTS

PL acknowledges support from The Heine Institute for Theoretical Physics, The National Security Agency, The Army Research Office and The Disruptive Technologies Office. ES acknowledges support from EU EuroSQIP and DFG SFB 631 projects.

[1] J.M. Raimond, M. Brune, and S. Haroche, Rev. Mod. Phys. 73, 565 (2001); H. Mabuchi and A.C. Doherty, Science 298, 1372 (2002).

[2] M.A. Nielsen and I.L. Chuang, Quantum Computation and Quantum Information (Cambridge University Press, Cambridge, 2000).

[3] E. Hagley, X. Maitre, G. Nogues, C. Wunderlich, M. Brune, J.M. Raimond, and S. Haroche, Phys. Rev. Lett. 79, 1 (1997).

[4] B.B. Blinov, D.L.M. Oehring, L.-M. Duan, and C.M.尊, Nature 428, 153 (2004); J. Volz, M. Weber, D. Schlenk, W. Rosenfeld, J. Vrana, K. Saucke, C. Kurtseifer, and H. Walnauer, Phys. Rev. Lett. 96, 030404 (2006).

[5] E.T. Jaynes and F.W. Cummings, Proc. IEEE 51, 89 (1963).

[6] M. Brune, E. Hagley, J. Dreyer, X. Maitre, A. Maali, C. Wunderlich, J.M. Raimond, and S. Haroche, Phys. Rev.

Lett. 77, 4887 (1996); B.T.H. Varcoe, S. Brattke, M. W eidinger, H.W. alther, Nature 403, 743 (2000).

[7] D. M eschede, H. W alther, and G. M uller, Phys. Rev. Lett. 54, 551 (1985).

[8] K. A n, J.J. C hilds, R.R. D esari, and M. F eld, Phys. Rev. Lett. 73, 3375 (1994); W. C hoi, J.-H. L ee, K. A n, C. F ang-Yen, R.R. D asari, and M.S. F eld, Phys. Rev. Lett. 96, 093603 (2006).

[9] G.R. G uthorlein, M.K. E ller, K.H. A yasaka, W. L ange, and H.W. alther, Nature 414, 49 (2001).

[10] S. N ussm ann, K. M urr, M. H ijkem a, B. W eber, A. K uhn, and G. R empe, N ature P hysics 1, 122 (2005).

[11] J.M. C k eever, A. B oca, A.D. B oozer, J.R. B uck, and H.J. K imble, N ature 425, 268 (2003).

[12] Y. M u and C.M. S avage, Phys. Rev. A 46, 5944 (1992); C. G inzel, H.-J. B riegel, U. M artini, B.-G. E nglert, and A. S chenzle, Phys. Rev. A 48, 732 (1993); T. P ellizzari and H. R itsch, Phys. Rev. Lett. 72, 3973 (1994); M. L o er, G.M. M eyer, and H.W. alther, Phys. Rev. A 56, 3923 (1997).

[13] M. B rune, F. S chmidt-K aeler, A. M aali, J. D reyer, E. H a gley, J.M. R aimond, and S. H aroche, Phys. Rev. Lett. 76, 1800 (1996).

[14] L.G. Lutterbach and L. D avidovich, Phys. Rev. Lett. 78, 2547 (1997).

[15] P. B ertet, A. A u eves, P. M aioli, S. O snaghi, T. M eunier, M. B rune, J.M. R aimond, and S. H aroche, Phys. Rev. Lett. 89, 200402 (2002).

[16] J. G ea-B anacloche, Phys. Rev. A, 44, 5913 (1991).

[17] A. A u eves, P. M aioli, T. M eunier, S. G leyzes, G. N ogues, M. B rune, J.M. R aimond, and S. H aroche, Phys. Rev. Lett. 91, 230405 (2003).

[18] G. M origi, E. S olano, B.-G. E nglert, and H. W alther, Phys. Rev. A 65, 040102 (2002).

[19] P. A lsing and H.J. C armichael, Quantum Opt. 3, 13 (1991); H. M abuchi and H.M. W iseman, Phys. Rev. Lett. 81, 4620 (1998); J.E. R einer, H. W iseman, and H. M abuchi, Phys. Rev. A 67, 042106 (2003).

[20] H. N ha and H.J. C armichael, Phys. Rev. Lett. 93, 120408 (2004).

[21] J. G ea-B anacloche, T.C. B urt, P.R. R ice, and L.A. O rozco, Phys. Rev. Lett. 94, 053603 (2005).

[22] E. S olano, G.S. A garwal, and H. W alther, Phys. Rev. Lett. 90, 027903 (2003).

[23] P. Lougovski, F. C asagrande, A. L ulli, B.-G. E nglert, E. S olano, and H. W alther, Phys. Rev. A 69, 023812 (2004); F. C asagrande, B.-G. E nglert, P. Lougovski, A. L ulli, E. S olano, and H. W alther, Opt. Spectrosc. 99, 301 (2005).

[24] P. Lougovski, E. S olano, and H. W alther, Phys. Rev. A 71, 013811 (2005).

[25] F. C asagrande and A. L ulli, Eur. Phys. J. D 36, 123 (2005); F. C asagrande and A. L ulli, J. Opt. B: Quantum Sem iclass. Opt. 7, S437 (2005).

[26] A.B. K limov, L.L. S anchez-Soto, A. N avarro, and E.C. Yustas, J. Mod. Opt. 49, 2211 (2002).

[27] C.C.Gerry and P.L. Knight, Introductory Quantum Optics (Cambridge University Press, Cambridge, 2005).

[28] Y. D alibard, Y. C astin, and K. M unier, Phys. Rev. Lett. 68, 580 (1992).